Fueling biomass-degrading oxidative enzymes by light-driven water oxidation

Bissaro, Bastien; Forsberg, Zarah; Ni, Yan; Hollmann, Frank; Vaaje-Kolstad, Gustav; Eijsink, Vincent G H

DOI
10.1039/c6gc01666a

Publication date
2016

Document Version
Accepted author manuscript

Published in
Green Chemistry

Light-driven water oxidation to fuel enzymatic conversion of biomass

Bastien Bissaro[a,b*], Zarah Forsberg[b], Yan Ni[c], Frank Hollmann[c], Gustav Vaaje-Kolstad[b], and Vincent G.H. Eijsink[b]

a. INRA, UMR792, Ingénierie des Systèmes Biologiques et des Procédés, F-31400 Toulouse, France
b. Department of Chemistry, Biotechnology and Food Science, Norwegian University of Life Sciences (NMBU), P.O. Box 5003, N-1432 Aas, Norway
c. Department of Biotechnology, Delft University of Technology, Julianalaan 136, Delft 2628BL, The Netherlands.

*Corresponding author:
bastien.bissaro@nmbu.no

Graphical Abstract

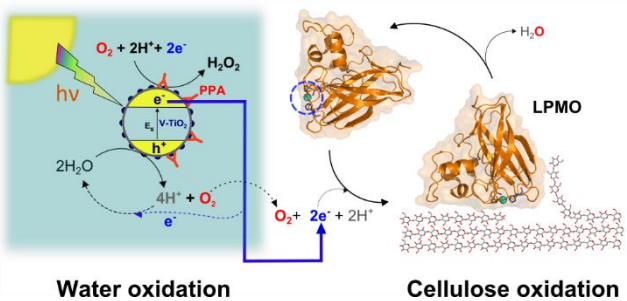

Schematic representation of light-driven reduction of LPMOs. Visible light is absorbed by the V-TiO_2 photocatalyst resulting in hole (h^+)-electron (e^-) pair separation and leading to O_2 production from water splitting. In the absence of an electron acceptor and depending on the conditions, subsequent oxygen reduction will generate H_2O_2 or regenerate H_2O. Polyprotic acids (PPA, red "antigen"-shape) are thought to be involved in shifting O_2 reduction towards H_2O instead of H_2O_2. Here, we show that the generated electrons can reduce the LPMO active site copper (blue dashed circle) in the absence of a redox mediator. This initiates the LPMO catalytic cycle, leading to oxidative cleavage of polysaccharides (right figure). The orange protein structure represents the *Streptomyces coelicolor* AA10 LPMO, *Sc*LPMO10C (PDB 4OY7). The interaction of the protein with cellulose (lower right panel) has not been mapped experimentally and the picture is shown for illustrational purposes only.

ABSTRACT

Photosynthesis entails the light-driven oxidation of water and subsequent use of the generated reducing equivalents for synthetically useful reactions. The transposition of this principle to *in vitro* controlled biocatalytic reactions is poorly studied. Here we demonstrate that light-driven oxidation of water catalysed by vanadium-doped TiO_2 (V-TiO_2) can fuel the activity of lytic polysaccharide monooxygenases (LPMOs), which are recently discovered key enzymes in biomass processing that depend on an external electron source for activity. This finding bridges the gap between photocatalysis and biomass decomposition, two important fields in the transition towards a bio-economy. Furthermore, this is the first demonstration of direct electron transfer from V-TiO_2 particles to a redox enzyme, expanding the repertoire of known photobiocatalytic reactions. Notably, this photobiocatalytic system allows control of LPMO activity in the absence of reducing agents or redox mediators, thus offering new tools for mechanistic studies of these important enzymes.

Key words: Lytic polysaccharide monooxygenases, Water oxidation, Titanium dioxide, Biomass, Photobiocatalysis

Abbreviations:
Aldonic acid form of oxidized oligosaccharide (AA); auxiliary activity family 9 or 10 (AA9 or AA10); cellobiose dehydrogenase from *Myriococcum thermophilum* (*Mt*CDH); cellobionic acid (GlcGlc1A); degree of polymerization (DP); electron/hole (e^-/h^+); lactone form of oxidized oligosaccharide (Lac); lytic polysaccharide monooxygenases (LPMOs); phosphoric acid swollen cellulose (PASC); polyprotic acid (PPA); reactive oxygen species (ROS); vanadium-doped titanium oxide (V-TiO_2)

The deconstruction of recalcitrant polysaccharides such as chitin[1] or cellulose[2–4], but also hemicellulose[5] or starch[6], was recently demonstrated to involve the oxidative action of enzymes named lytic polysaccharide monooxygenases (LPMOs). These carbohydrate active enzymes, whose discovery has had profound impact on our perception of enzymatic biomass conversion, are currently classified in four families of Auxiliary Activities (AA); AA9, 10, 11 and 13. LPMOs are copper-dependent enzymes[3,4] that catalyze the oxidation of glycosidic bonds via a still unclear mechanism[7,8], involving molecular oxygen and externally provided electrons that can be supplied by various small organic compounds (e.g. ascorbic acid), by proteins (e.g. cellobiose dehydrogenase, CDH) or by highly reduced polymers such as lignin[9,10]. It has been suggested that CDH is the natural electron provider for fungal LPMOs (AA9, 11 and 13)[4,11]. A functionally similar redox protein has not yet been identified for bacterial LPMOs (AA10). Controlling the flow of electrons to the LPMO is crucial for a well-functioning catalytic system since both LPMOs and CDHs form reactive oxygen species (ROS) in the absence of substrate[12,13] that may be deleterious for overall process efficiency. Furthermore, from an applied standpoint, the use of costly and often enzyme-specific co-factors or mediators involved in electron chains (e.g. NADH, flavins), represents a substantial technical and economic challenge. (Poly)ols such as ethanol or glucose, or formic acid can be used to indirectly regenerate monooxygenases via reduced nicotinamide cofactors[14]. These methods, however, are prohibitively complex (due to the use of multiple enzymes), expensive and atom-inefficient if at-scale applications of LPMOs are envisioned.

Looking for alternative electron supply systems, we drew our attention to using water as cheap and readily available electron donor. Liberation of reducing equivalents from water poses major thermodynamic and kinetic challenges. In Nature these challenges are met by exploiting light, an abundant energy source that has been harvested by living organisms for billions of years in photosynthesis, i.e. by conversion of photon energy to chemical energy. Over the past century, attempts have been made to explore this energy source in organic synthesis[15], in what today is a sub-branch of chemistry called photochemistry or photocatalysis. Inspired by Nature, and building on progress in photochemistry, a new field called photobiocatalysis is now emerging, where the focus is on harnessing the power of sunlight to trigger biochemical processes and perform a range of enzymatic reactions under eco-friendly conditions. So far, only a few examples of successful photobiocatalysis have appeared in the literature[16]. As a key example, it was recently shown that by using vanadium-doped titanium dioxide (V-TiO_2) and flavin redox mediators, it was possible to drive the enantiospecific reduction of ketoisophorone to (R)-levodione by a reductase[17]. These are interesting developments since, on one hand, TiO_2 constitutes one of the best-studied, cheap and robust inorganic water oxidation catalysts[18,19], while, on the other hand, these catalysts may allow tight control of an ubiquitous class of enzymes, namely redox enzymes, that carry out very powerful chemistry.

In this study, we set out to explore the potential of photobiocatalysis in biomass conversion by supply of reducing equivalents to LPMOs. We envisioned a photobiocatalytic system wherein V-TiO_2-mediated and visible light-driven oxidation of water would be coupled to LPMO-catalyzed oxidative degradation of recalcitrant, insoluble polysaccharides such as cellulose (Scheme 1). Importantly, our experimental system allowed demonstrating that electrons generated at the V-TiO_2 particles can be transferred to the enzymes without the use of a redox mediator, which has important implications for further developing the field of photobiocatalysis. This electron-donating system offers unprecedented spatio-temporal control of electron delivery to LPMOs, opening up new ways to control enzymatic conversion of biomass and to study the mechanism of these crucial enzymes.

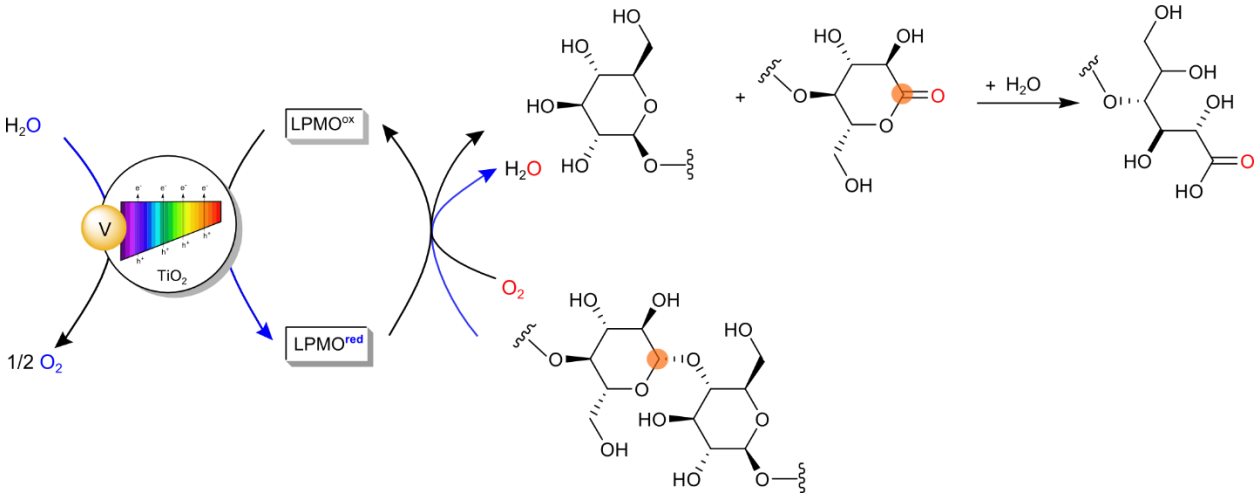

Scheme 1 | Proposed photobiocatalytic oxidation of glycosidic bonds using an LPMO. The reductive activation of molecular oxygen on the LPMO occurs via direct reduction of LPMO-bound Cu(II). The reducing equivalents required for this are derived from V-TiO_2-mediated and light-promoted oxidation of water. Blue arrows indicate

the suggested flow of reducing equivalents (electrons) and their sources. The oxygenation leading to cellulose chain cleavage occurs at the C-1 position (orange circle) of the D-glucose unit and the resulting lactone is then spontaneously hydrolysed (in a pH-dependent manner) into the corresponding aldonic acid.

RESULTS

Proof-of-concept

As a proof-of-concept experiment, a cellulose-active AA10-type LPMO from *Streptomyces coelicolor* (*Sc*LPMO10C, also known as CelS2) was mixed with a crystalline substrate (Avicel) and V-TiO_2, and the resulting reaction mixture was exposed to visible light (λ > 400 nm). Generation of soluble cello-oligomers in their aldonic acid form, the primary products of LPMOs oxidizing the C-1 carbon, was indeed observed (**Fig. 1a**) and the reaction proceeded linearly without apparent reduction of the initial product formation rate for at least 22 h (**Fig. 1b**). In the absence of either the photocatalyst (V-TiO_2), or light no soluble products were observed (**Fig. 1b)**. The overall rate of the reaction was approximately 35% of the rate obtained when using ascorbic acid as sacrificial electron donor. The product profile obtained in the new photoenzymatic reaction was comparable to that obtained when using ascorbic acid (**Fig**. **1a**), but showed a higher presence of side products. Since the LPMO contains a copper ion binding site with a K_d in the nanomolar range[20], addition of enzyme to a reaction mixture generates a low concentration of free Cu(II) ions, which in the presence of H_2O_2 generated at the V-TiO_2 catalyst could lead to cellulose oxidation by Fenton-like chemistry[21,22]. Additional control experiments in which the enzyme was replaced by various concentrations of Cu(II)SO_4 (0 to 1000 µM) did not show any sign of Fenton-like chemistry taking place (**Supplementary Fig. 1**).

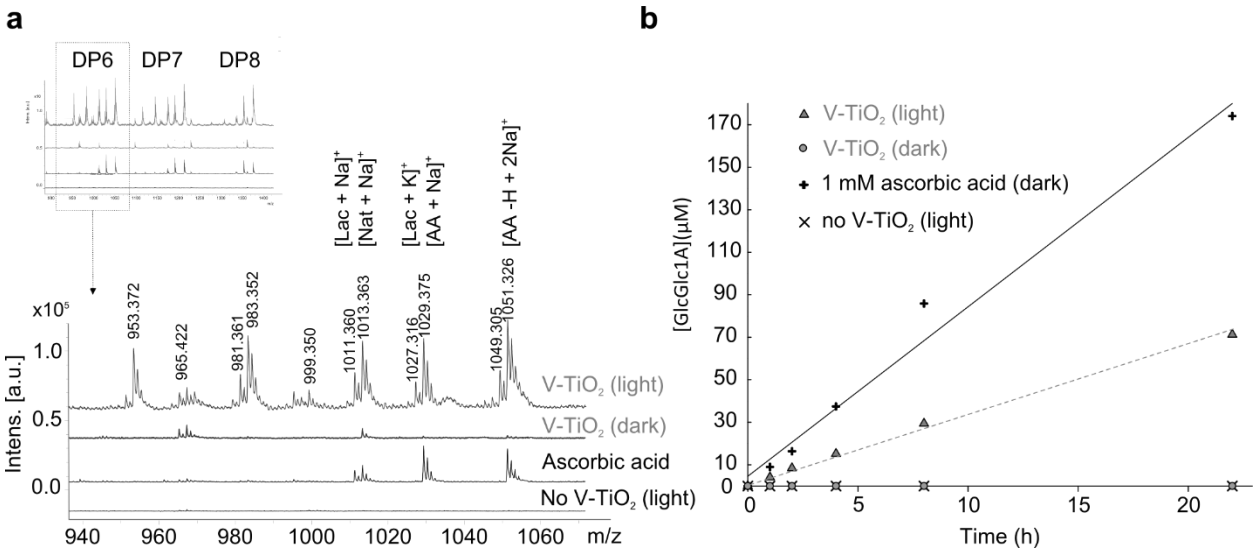

Figure 1 | Proof-of-concept for photobiocatalytic oxidation of cellulose. (a) MALDI-TOF MS analysis of products generated from Avicel (10 $g.L^{-1}$) by *Sc*LPMO10C (0.9 µM) after 22 h of incubation. Reactions were carried out in sodium phosphate buffer (50 mM, pH 6.0) at 40 °C, under magnetic stirring. Reaction conditions varied in terms of exposure to visible light (I = 10%; I_{max}, approx. 16.6 $W.cm^2$), the presence of ascorbic acid (1 mM) and the presence of V-TiO_2 (10 $g.L^{-1}$). The figure shows the DP6 – DP8 region as well as an enlargement of the DP6 region. The abbreviations indicate sodium or potassium adducts of native (Nat) or oxidized oligosaccharide in the lactone form (Lac) or the aldonic acid form (AA). Note that the 1051 signal is diagnostic of aldonic acids, since the introduced

carboxyl group is needed to obtain double sodium adducts. **(b)** Time-course for the release of aldonic acid products from Avicel by *Sc*LPMO10C corresponding to reactions described in panel **(a)**. Before product quantification, the soluble products were hydrolyzed using an endoglucanase, *Tf*Cel5A, yielding oxidized products with a degree of polymerization (DP) of 2 or 3 (GlcGlc1A, $(Glc)_2Glc1A$) in approximately equal amounts, that were quantified by HPAEC-PAD analysis using corresponding standards. Only production of GlcGlc1A is shown.

Studies with LPMOs from another family (AA9), with other substrate specificity (chitin) and with another oxidative regioselectivity (C-1/C-4) showed that the photoenzymatic systems is generally applicable since oxidized oligomeric products were observed in all cases (**Supplementary Fig. 2**). **Supplementary Fig. 3** shows that the system is not limited to artificial light sources used under laboratory conditions, but that also natural sunlight efficiently promoted the reaction.

Further characterization of the photoenzymatic reaction system

Encouraged by the promising proof-of-concept experiments we set off to gain further insight into the rate-limiting parameters of the photobiocatalytic system. Particularly, the influence of light intensity and the concentrations of V-TiO_2 and *Sc*LPMO10C on the reaction speed was investigated (**Fig. 2**). A positive correlation between the overall rate and the concentration of the water oxidation catalyst (V-TiO_2) was indeed observed (**Fig. 2a**). The intensity of the light source, on the other hand, had no significant influence on the overall rate (**Fig. 2b**). These observations suggest that the thermodynamically challenging water oxidation step is rate-limiting, a notion that was supported by the observation that higher reaction rates were obtained when using more easily oxidizable sacrificial electron donors such as formate or methanol (**Supplementary Fig. 4**). In terms of biocatalyst concentration the system was well-behaved exhibiting a linear correlation between [*Sc*LPMO10C] and the product formation rate (**Fig. 2c**), which suggests that the efficiency of water oxidation is correlated with the presence of the LPMO as electron acceptor, as discussed further below. It is worth noting that all standard reactions were performed at saturating substrate concentrations (**Supplementary Fig. 5)**, as corroborated by the fact that linear kinetics were obtained in all conditions**.**

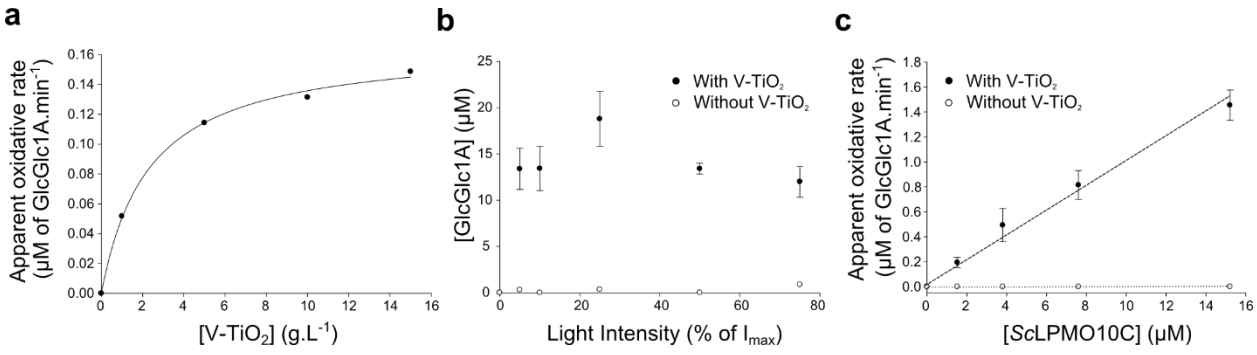

Figure 2 | Influence of (a) [V-TiO_2], (b) light intensity and (c) [*Sc*LPMO10C] on reaction efficiency. All reactions were carried out at 40 °C, in sodium phosphate buffer (50 mM, pH 6.0) with Avicel (10 $g.L^{-1}$). When they were not the variable under study, light intensity (λ > 400 nm), [*Sc*LPMO10C] or [V-TiO_2] were kept constant at I = 25%.I_{max}, 1.5 µM and 10 $g.L^{-1}$ (for **b**) or 5 $g.L^{-1}$ (for **c**), respectively. The values plotted reflect product concentrations after 2 h reactions for **(b)** and reaction rates derived from 4 h time-course monitoring for **(a)** and **(c)**. Error bars in **(b)** and **(c)** show ± s.d. (n =3).

In the course of the characterization of this [*hv*/V-TiO_2/LPMO] system it was noticed that the presence of phosphate ions had a positive influence on the overall rate of the reaction (**Supplementary Fig. 6**). Possibly, this can be assigned to a decreased formation of ROS such as H_2O_2 as previously described by Sheng and coworkers[23], who showed that polyprotic acids (PPA) modulate oxygen reduction pathways at the TiO_2 surface. In agreement with the findings by Sheng et al., replacing phosphate by glutamate or malonate, two alternative PPAs, also allowed the photobiocatalytic oxidation of cellulose to proceed (**Supplementary Fig. 7**). The use of a monoprotic acid (acetic acid) gave low and unstable oxidation rates, suggesting that redox side reactions occur, perhaps involving H_2O_2 or ROS generated at the V-TiO_2 surface (**Supplementary Fig. 7**). Thus, our data confirm that PPA, and phosphate in particular, positively influence the competition between ROS-generating reduction of O_2 and reduction of the LPMO.

LPMO activity can be controlled by a light switch

To further investigate the controllability of the photobiocatalytic system, we investigated the activation and deactivation of the system by manipulation of the light source. After a period of illumination of 2 h, allowing the enzyme to initiate the oxidation of cellulose, the oxidation rate was significantly reduced (approx. 80% less) when the light was turned off compared to a control reaction where the light was kept on (**Fig. 3**). It is noticeable that the reaction does not stop immediately after the light has been switched off (see below for further discussion). Expectedly, when the light was switched on again the oxidation rate was restored to a value equivalent to that measured in the first "light on" phase.

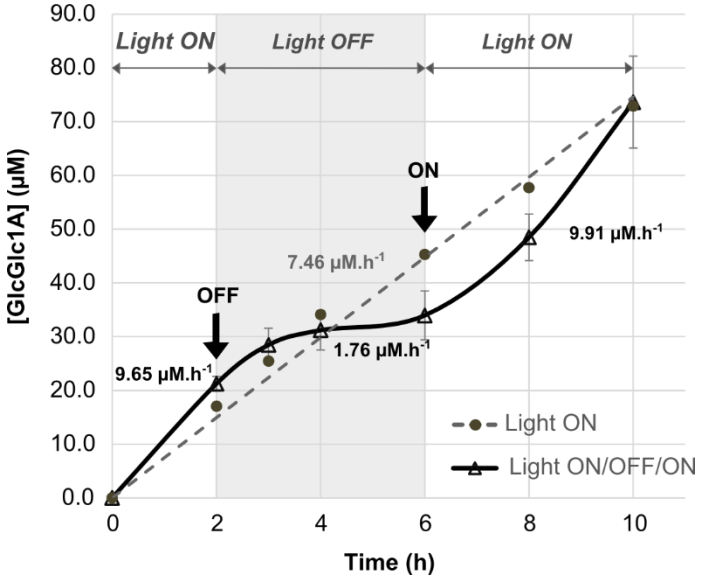

Figure 3 | Impact of a light/dark cycle on the *hv*/V-TiO_2/ LPMO photobiocatalytic system. The figure shows a time-course for oxidation of Avicel (10 $g.L^{-1}$) by *Sc*LPMO10C (1 µM) in the presence of V-TiO_2 (5 $g.L^{-1}$). Before quantification, soluble products were hydrolyzed by *Tf*Cel5A, yielding oxidized products with a degree of polymerization of 2 or 3 (GlcGlc1A, $(Glc)_2Glc1A$). Reactions were carried out in sodium phosphate buffer (50 mM, pH 6.0) at 40 °C under magnetic stirring and exposed to visible light at an intensity of 25% of maximum intensity (approx. 42 $W.cm^2$). Derived cellobionic acid release rates are plotted on the graph for each light phase (9.65, 1.76

and 9.91 μM.h^{-1}, for ON, OFF and ON phases respectively) as well as for the reaction kept constantly under light exposure (7.46 μM.h^{-1}). Error bars show ± s.d. (n =3).

New insight into the spatio-temporal origin of electrons involved in the LPMO mechanism

In addition to its potential practical value (i.e. making water available as sacrificial electron donor to decompose polysaccharides), the V-TiO_2 system also offers new possibilities to investigate the LPMO mechanism. The heterogeneous nature of the electron supply system allows for dissection of the reductive half-reaction (LPMO-Cu(II) to LPMO-Cu(I)) from the oxidative half reaction (i.e. cellulose oxidation) by physical separation of the V-TiO_2 photocatalyst from the enzymes and by removing the light source (as demonstrated by the switch on/off experiment). To explore this opportunity further, we carried out experiments consisting of the following steps: (1) reduction of the LPMO-Cu(II) by photocatalytically generated electrons, under low oxygen concentrations (i.e. N_2-flushed), (2) separation of the LPMO from the electron source (i.e. the V-TiO_2 photocatalyst), (3) detection of the reduced state of the LPMO, (4) use of the pre-reduced LPMO for cellulose oxidation.

It is generally thought that in the initial phase of catalysis, the reduced LPMO-Cu(I) reacts with O_2 in a one-electron reduction step leading to formation of LPMO-Cu(II)-O_2^{-}[8]. The formation of this redox intermediate can be monitored indirectly by measuring the production of oxidized substrate or, in the absence of substrate, H_2O_2, processes that, notably, require transfer of a second electron. Reduction (LPMO-Cu(II) to LPMO-Cu(I) step) may also be monitored directly by measuring absorbance in the visible range (615-650 nm), but this method is insensitive and requires high protein concentrations (> 500 μM). We show here that fluorescence is better suited for monitoring the redox state of an LPMO offering higher sensitivity and a time-scale that is compatible with LPMO re-oxidation kinetics at low, realistic, enzyme concentrations (1-5 μM). This novel method was used to probe the reduction of the copper center by the *hv*/V-TiO_2 system (**Fig. 4**).

A positive control reaction revealed an increase in fluorescence of the copper-saturated *Sc*LPMO10C upon addition of ascorbic acid (**Fig. 4d**), as previously observed for laccases[24] or tyrosinases[25]. Pre-activation experiments with *Sc*LPMO10C-Cu(II) (i.e. steps 1 – 2 described above) showed that the *hv*/V-TiO_2 system led to a similar increase in LPMO fluorescence (**Fig. 4d**), clearly showing that the *hv*/V-TiO_2 system leads to reduction of the copper and that this reduction can be observed in a situation where the LPMO has been separated from the reductant. A control experiment showed that the enzyme was reduced to only a very small extent by V-TiO_2 when not exposed to light. Another control experiment showed that the protocol employed was efficient in separating the electron source from the LPMO since hardly any increase in fluorescence was observed when the supernatant of a light-exposed V-TiO_2 suspension was mixed with fresh unexposed *Sc*LPMO10C-Cu(II). **Supplementary Fig. 8** shows that this fluorescence method also works for monitoring reduction by other reducing agents, such as L-cysteine, 1,4-dithiothreitol (DTT), or more complex electron-donating systems such as cellobiose dehydrogenase/lactose. Importantly, the fluorescence approach also yielded visualization of the decay of the reduced LPMO intermediate (**Fig. 4d; Supplementary Figure 8**). While decay curves for ascorbic acid, quite remarkably did not lead to restoring the LPMO "ground state", clean exponential decay curves back to the ground state could be generated using the *hv*/V-TiO_2 system, highlighting the usefulness of separating the electron source from the reduced LPMO (**Fig.4a-c**). Using theoretical fitting

to a single-exponential decay model, as explained in **supplementary text 1**, a half-life of 36 min was derived and the rate constant for the decay was calculated to be approximately 0.02 min^{-1}, which in the same order of magnitude as the rate of H_2O_2 production by LPMOs that are incubated with a reductant in the absence of substrate (Kittl et al., 2012[12]; see below).

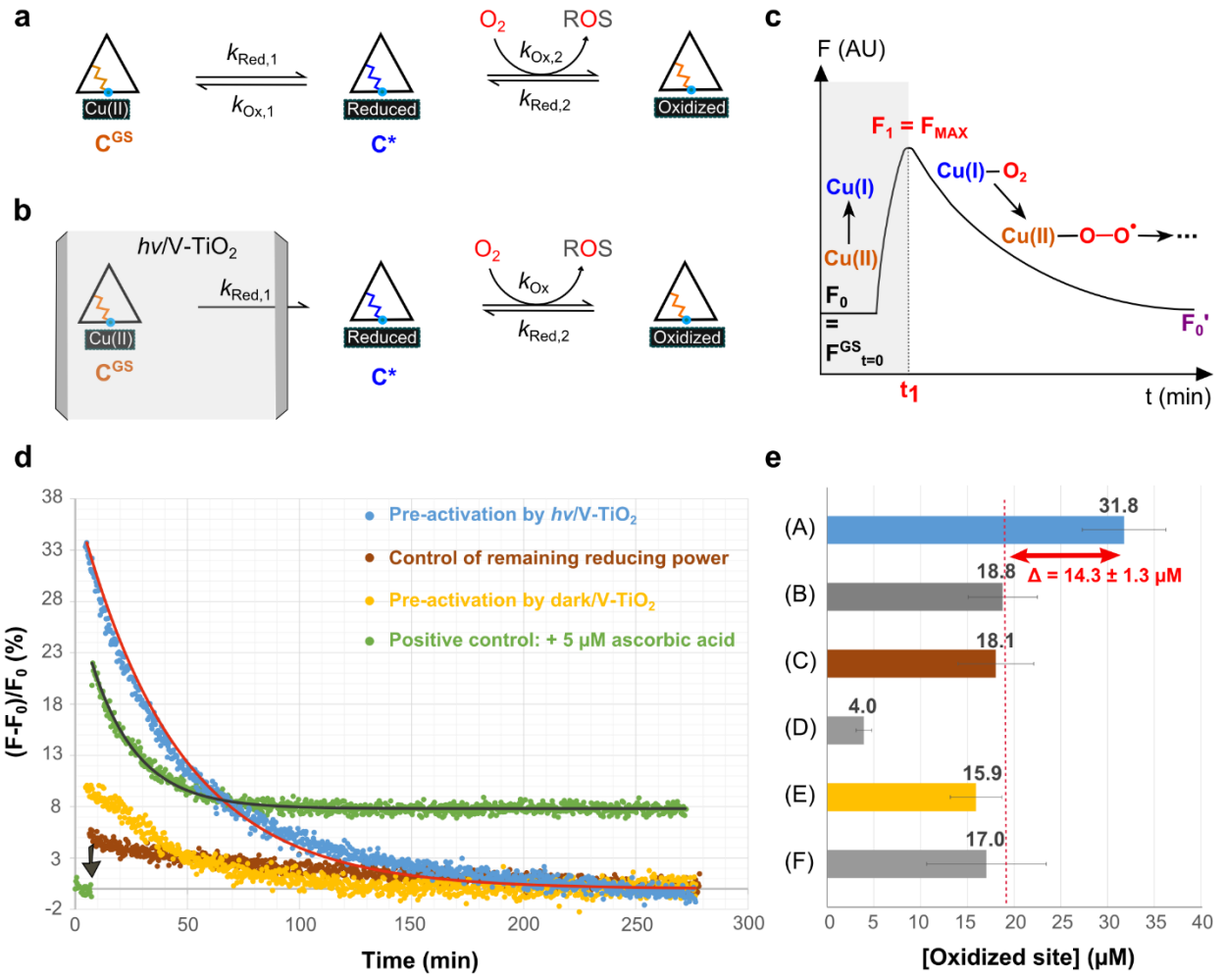

Figure 4 | Probing the formation of an LPMO redox intermediate by photocatalytic reduction and determination of its life-time by fluorescence spectrophotometry. (a) A simplified model of reduction and oxygen-mediated re-oxidation of the LPMO copper center. **(b)** When using *hv*/V-TiO_2 as a generator of reducing power, the latter can be removed (grey shading) from the reaction medium before fluorescence monitoring which simplifies the observation of subsequent decay of the reduced complex (C* species). **(c)** The LPMO-Cu(II) complex (C^{GS}) displays an intrinsic ground state fluorescence (F^{GS} corresponding to the total fluorescence before reduction, i.e. F_0). Upon reduction, modification of the electronic environment of aromatic amino acids close to the copper center induces an increase in fluorescence towards a maximum value (F_1)[24]. The reduced state of the LPMO (C*, assumed to represent the LPMO-Cu(I) state, although it could be another reduced intermediate) is not stable and undergoes re-oxidation by molecular oxygen towards a more stable state with a decay rate constant k_{Ox} in the order of 0.02 min^{-1} (see **Supplementary text 1**). F_0' is the fluorescence measured once the system is stabilized and is equal to F_0 if the ground state is fully restored, as is the case only for the *hv*/V-TiO_2-fueled reaction. **(d)** Relative fluorescence intensity variation of *Sc*LPMO10C after being exposed to *hv*/V-TiO_2 (blue dots) or dark/V-TiO_2 (yellow dots). Negative and positive controls consist in adding either the supernatant of a light-exposed V-TiO_2 suspension

(brown dots) or ascorbic acid (green dots) to a solution of *Sc*LPMO10C not exposed to light. **(e**) Quantification of oxidized sites (GlcGlc1A and $(Glc)_2Glc1A$) introduced in PASC by *Sc*LPMO10C (7 µM) after pre-activation by *hv*/V-TiO_2 (reaction A, equivalent to blue dots of panel **d**). As shown in detail in **supplementary Fig. 9** several control reactions were carried out showing the absence of remaining reducing power in the supernatant of a light-exposed V-TiO_2 suspension in which free copper (5 µM) was added (reaction B) or not (reaction C). The cellulose-oxidizing potential of the supernatants of a light-exposed V-TiO_2 suspension (reaction D) and of unexposed V-TiO_2 /*Sc*LPMO10C (reaction E) or *Sc*LPMO10C (reaction F) solutions was also assessed. The number of oxidized sites observed for reaction D is in the error range of the value obtained for untreated PASC solutions (83 ± 5 µM). The (similar) numbers of oxidized sites in control reactions B, C, E and F show how much oxidation of PASC *Sc*LPMO10C can accomplish in the absence of an electron donor. For reactions described in panel **(d)** and **(e)**, there is a 5 min delay between the light treatment and subsequent fluorescence data acquisition **(d)** or addition to PASC **(e)**, which is the time needed to separate the enzyme from the electron source. For reactions with ascorbic acid (added at the arrow), constant fluorescence monitoring was possible. Error bars in **(e)** show ± s.d. (n =3).

Knowing that a relatively stable redox intermediate could be obtained using the pre-activation of LPMOs by *hv*/V-TiO_2 and that efficient separation of the LPMOs from its electron source was possible, novel studies for obtaining mechanistic insights into LPMOs could be envisioned. As a first proof of principle, we used the system to obtain a glimpse of the order of molecular events, in particular electron delivery, during LPMO action. Experiments were set up according to steps 1 – 4 described above, meaning that after reduction of the LPMO and separation from the electron source, the "pre-activated" LPMO was incubated with cellulose (**Fig. 4e and Supplementary Fig. 9**). A series of control reactions (**Fig. 4e**, reactions B,C,E & F; see **Supplementary Fig. 9** for more details) showed similar product levels, reflecting the level of cellulose oxidation that is accomplished by *Sc*LPMO10C in the absence of pre-activation or an electron donor and also showing that the enzyme remained catalytically competent under all conditions used. This low activity in the absence of reductant is attributed to the presence of reducing power in the substrate (chemical compounds or reducing ends), as observed in previous studies[1,26]. Importantly, pre-activation of the LPMO consistently led to increased product levels (**Fig. 4e,** reaction A). The additional product formation in reaction A corresponds to 14.3 µM, which, considering that the enzyme concentration was 7 µM, leads to a ratio of 2.0 ± 0.3 additional cuts per enzyme.

Importantly, these pre-activation experiments, which were conducted under "minimal" conditions (water, phosphate, V-TiO_2, light and enzyme) provide further and convincing proof of light-driven, V-TiO_2-catalyzed water oxidation being the source of the electrons that drive LPMO activity.

DISCUSSION

To the best of our knowledge, the present study provides the first example of a light-to-chemical energy conversion pathway that can be utilized for the controlled deconstruction of recalcitrant polysaccharides. We show that photo-generated electrons coming from water oxidation can fuel a variety of LPMOs, allowing these enzymes to carry out oxidative cleavage of glycosidic bonds in substrates such as chitin and cellulose. Following proof-of-concept experiments, we carried out a thorough characterization of the [*hv*/V-TiO_2/LPMO] system, revealing critical parameters as well as applications towards controlling and understanding LPMO functionality.

Water splitting on irradiated TiO_2 nanoparticles was discovered in 1972[27] and has been explored in a variety of chemical reactions[15]. However, the direct use of electrons generated by light-induced water oxidation to drive enzyme-catalyzed redox reactions was only recently reported[17]. In this latter study an electron carrier was used to ensure electron transport between both entities and the need for such carriers, for example NADPH or flavins is considered as both a technological and economic obstacle in development of photo-biocatalytic systems[16]. Importantly, the present study provides the first example of light-driven enzyme catalysis without the need for a redox mediator.

From a thermodynamic standpoint, water oxidation is very challenging (E^0_{ox} = -1.23 V for H_2O/O_2) and is often considered as the rate-limiting step in TiO_2-photocatalyzed reactions. This also seems to be the case for the present photobiocatalytic system, since we observed rate enhancements when using alternative sacrificial more easy-to-oxidize electron donors such as methanol or formate (**Supplementary Fig. 4**). Interestingly, while water oxidation is likely to be rate-limiting, an increase in LPMO (= electron acceptor) concentration led to an increase in the cellulose oxidation rate (**Fig. 2**). It is noteworthy that the "rate-limiting" step (water oxidation) is intimately related to and influenced by its couterpart reaction (e^-/h^+ pair generation) that is bidirectional (e^-/h^+ recombination can occur in parallel). It is therefore plausible that increasing the LPMO concentration tips the balance in favor of e^- transfer towards the protein electron acceptor (the LPMO) versus direct reduction of O_2 or e^-/h^+ recombination, thus increasing the overall apparent oxidation rate of cellulose.

In line with existing data on TiO_2 technology[23,28–30], we demonstrate that the performance of the photocatalyst is affected by phosphate or other poly-protic acids, that are not necessary for the LPMO to carry out its oxidative role in standard reactions. Several studies have revealed that phosphate from aqueous medium absorbs onto the TiO_2 surface[28], in an ionic strength-dependent manner[31] and can provide a proton relay allowing to switch from single electron reduction transformations (O_2 to H_2O_2 pathway) to a $4e^-/4H^+$ path (conversion of O_2 into H_2O)[23].

The photo-biocatalytic concept reported in this study opens new and exciting perspectives. The *hv*/V-TiO_2 system enables light-mediated control of LPMO activity, in the absence of any other reducing agent, as shown by the light "ON/OFF" experiment (**Fig. 3**). Studies of the synergy between glycoside hydrolases (GHs) and LPMOs could benefit from this novel tool, since LPMO activity now can be tightly regulated, in any phase of the polysaccharide deconstruction process. Regulating the activity of LPMOs that are recognized as potential virulence factors could provide new insights into pathogenic processes[32]. From a more applied standpoint, one could envisage the use of the *hv*/V-TiO_2 system in novel approaches to polysaccharide fiber engineering[33] by monooxygenases. Conceivably, better control of the duration and timing of LPMO activity on cellulose, or other substrates, will afford a better control of oxy-functionalisation[34] and should expand the possibilities of design of new (bio-inspired) materials.

Importantly, due to progress in the field of material science, potentially better photocatalysts are emerging with improved quantum efficiency, and with improved control over side reactions occurring at the surface[35,36]. On paper, another advantage of the *hv*/V-TiO_2 technology is that water oxidation not only generates electrons but also O_2, which is a substrate of LPMOs. However, producing substantial levels of "free" O_2 from H_2O on TiO_2 surfaces is challenging[37]. Side reactions and e^-/h^+ recombination events tend to result in low O_2 levels. Indeed, the *hv*/V-TiO_2 system employed here did not yield detectable LPMO activity under anaerobic conditions. Interestingly, recent reports[37] describe cobalt-based photocatalysts that achieve higher O_2 production levels that might yield sufficient *in situ*

production of molecular oxygen to drive LPMO activity. The perspective of LPMO-catalyzed reactions in O_2-depleted or anaerobic conditions is of major interest, because oxygen may be limiting in industrial reactors, but also because this could potentially allow combining the power of LPMOs with that of anaerobic microorganisms (which lack LPMOs for obvious reasons).

The *hv*/V-TiO_2 photocatalytic system represents a unique electron source for LPMOs in the sense that it provides a means to separate the polysaccharide substrate from the electron source (by physical separation and switching off the light). The system could thus potentially be used to study the flow of electrons during catalysis, a topic that remains one of the mysteries of LPMO chemistry[38,39]. To study LPMO reduction in more detail we implemented a fluorescence method. When combined with the *hv*/V-TiO_2 system, we could observe LPMO reduction as well as a single exponential decay-type profile back to the initial ground state. It is well known that in the absence of substrate, the reduced LPMO undergoes a futile cycle by reacting with O_2 leading likely to H_2O_2 production[8,12]. Importantly, our data show that the decay of the intermediate does not require any externally added electron and the decay rate calculated from the fluorescence decay curves in **Fig. 4** (approx. 0.02 min^{-1}) is in good agreement with previously reported rates for H_2O_2 production by LPMOs in the absence of substrate (Kittl et al.[12]; the rates reported here are in the range 0.03 – 0.36 min^{-1}). It is also of interest to note that the decay rate in the absence of substrate is an order of magnitude lower than reported rates of substrate oxidation[1,40], which makes biological sense.

Oxidative cleavage of cellulose or chitin by an LPMO consumes two electrons. To get insight into where these electrons may come from, we carried out experiments with pre-activated LPMOs that had been separated from the electron source. We found that the pre-activated LPMO indeed could oxidize cellulose and that the number of additional oxidation reactions was in the order of two cuts per enzyme (reaction A, **Fig. 4e**). This is an intriguing finding, since it implies that each pre-activated LPMO, which would normally be assumed to carry one reducing equivalent in the form of Cu(I), on average contained or was able to recruit four electrons. Several scenarios for electron supply to LPMOs can be envisaged, including scenarios where the LPMO carries two reducing equivalents before encountering the substrate (See **Supplementary Fig. 10, "**pre-charged" model). Such scenario would be compatible with the observed decay of the redox intermediate that revealed to not require externally added electrons. However, in all scenarios, one would expect only one cleavage to occur per pre-activated LPMO. One possible explanation for the present finding is that the catalytic cycle initiated by the pre-activated LPMO once it binds productively to the substrate, unleashes oxidizing power in the catalytic center that is sufficient to attract electrons from reducing ends in the substrate or from sources not usually considered as reductants. Further investigations will be needed to confirm the finding from the pre-activation experiments, perhaps using other LPMOs and different substrates (e.g. clean soluble substrates). In this respect, we believe that the *hv*/V-TiO_2 photocatalytic tool presented here will be of great help in deciphering the mode of action of LPMOs, which are intriguing and powerful enzymes that are likely involved in many biocatalytic phenonema some of which are yet to be discovered or understood.

As one of the very first examples in this emerging field of science[41,17], the orchestration of chemical power and enzyme selectivity allowed us to harness light energy to use water as an electron source and activate monooxygenases for the deconstruction of recalcitrant polysaccharides. Current developments in both chemistry of photocatalysts and further understanding of monooxygenase action

will allow novel eco-friendly enzyme applications, using light as a universal source of energy, in the frame of a developing bio-economy.

ONLINE METHODS

Materials

The V-TiO_2 photocatalyst was prepared in-house (Delft University, Netherlands) according to a previously described protocol[42]. Ammonium vanadate (corresponding to a final 1% w/w V on TiO_2) was added to a solution of oxalic acid in water (pH 2.0) and heated gently to approx. 50 °C until a clear solution was obtained. To this mixture, TiO_2 (P25 from Evonik; particle size <25 nm) was added in portions followed by stirring for an additional hour. Afterwards, the solvent (water) was removed by heating up the mixture to 70 °C under reduced pressure, followed by an additional drying step at 110 °C for 24 h. Air calcination was achieved in a tubular furnace by heating up to 400 °C (10 °C min^{-1}) and maintaining the material at this temperature for 4 h. Most of the other chemicals were purchased from Sigma-Aldrich. β-chitin extracted from squid pen was purchased from France Chitin (Orange, France) and crystalline cellulose (Avicel PH-101) was purchased from Sigma.

Production and purification of recombinant LPMOs

Recombinant AA10 LPMOs from *Streptomyces coelicolor* (*Sc*LPMO10C and *Sc*LPMO10B) and from *Serratia marcescens* (CBP21) were produced and purified according to previously described protocols[20,26]. The recombinant fungal AA9 from *Phanerochaete chrysosporium* K-3 (*Pc*LPMO9D) was produced and purified as previously described[43]. All LPMOs used in this study were prepared in sodium phosphate (50 mM, pH 6.0), copper-saturated with Cu(II)SO_4 and desalted (PD MidiTrap G-25, GE Healthcare) before use.

Standard photobiocatalytic reaction

The photoreactor was a cylindrical glass vial (1.1 mL) with conical bottom (Thermo Scientific) and a 500 µL reaction volume. Typical reactions were carried out as follows: the enzyme (1-15 µM) and the substrate, Avicel (10 $g.L^{-1}$) or β-chitin (10 $g.L^{-1}$), were mixed in sodium phosphate buffer (pH 6.0, 50 mM) and incubated at 40 °C under magnetic stirring during 10 min. In the meantime a suspension of V-TiO_2 (50 $mg.mL^{-1}$) was prepared in water and added to the reaction mix (5 $mg.mL^{-1}$ final concentration), followed by incubation for 10 additional minutes. Then, the reaction was initiated by turning on the light source or by adding ascorbic acid (1 mM) for positive controls without V-TiO_2. The irradiation was performed top-wise (1 cm distance from liquid surface) using a 150 W, super-quiet xenon lamp with ozone-free bulb (total reflection type, code L9588-04, Hamamatsu Lightningcure LC8) and a 4-furcated fiber optic light guide (8A10014-35-0410, i.e. 1 m length, 3.5 mm diameter). The light was filtered thought a cutoff filter (λ>400 nm, 95 % transmittance, code A9616-09, Hamamatsu Lightningcure LC8). According to the manufacturer's data, the light intensity loss through the 1 meter 4-furcated fiber optic cable is 45%, resulting in 16 W being delivered to the liquid surface, assuming the shutter is fully open. For most of the experiments, the aperture was set to 25% (i.e. 4 W equivalent to an intensity of 42 $W.cm^2$).

At regular intervals, 55 µL samples were taken from the reaction mixtures and soluble fractions were immediately separated from the insoluble substrate and V-TiO_2 particles by filtration using a 96-well filter plate (Millipore) operated with a vacuum manifold. By separating soluble and insoluble

fractions, LPMO activity is stopped, as the LPMOs used in this study do not oxidize soluble cello-oligosaccharides. Filtered samples were frozen (-20 °C) prior to further analysis.

Analysis of reaction products

For qualitative analysis, samples were analysed by MALDI-TOF MS, as previously described[2]. Before quantification, solubilized cello-oligosaccharides were hydrolyzed with the endoglucanase Cel5A from *Thermobifida fusca* (*Tf*Cel5A), yielding glucose, cellobiose and oxidized products with a degree of polymerization of 2 or 3 (GlcGlc1A, $(Glc)_2Glc1A$). The products were separated by high performance anion exchange chromatography (HPAEC) and monitored by pulsed amperometric detection (PAD) using a Dionex Bio-LC equipped with a CarboPac PA1 column operated with a flow rate of 0.25 mL/min in 0.1 M NaOH (Eluent A) and a column temperature of 30 °C. Native and oxidized products were eluted and separated as previously described[44] using a stepwise gradient with increasing amount of eluent B (0.1 M NaOH + 1 M NaOAc), as follows: 0-10 % B over 10 min, 10-30 % B over 25 min, 30-100 % B over 5 min, 100-0 % B over 1 min, 0 % B over 9 min. For samples that had been treated with cellulases, containing only short products, a steeper gradient was used as follows: 0-10 % B over 10 min, 10-18 % B over 10 min, 18-30 % B over 1 min, 30-100 % B over 1 min, 100-0 % B over 0.1 min and 0 % B over 13.9 min. Oxidized dimers and trimers were quantified using GlcGlc1A and $(Glc)_2Glc1A$ standards obtained by incubating (40 °C, 1000 rpm) cellobiose (2 mM) or cellotriose (2 mM) with the cellobiose dehydrogenase from *Myriococcum thermophilum* (*Mt*CDH, 2 µM, 3 additions over 3 days to obtain maximum conversion of 95%). Under all conditions the amounts of oxidized dimer and trimer were similar (average molar ratio of 0.92 ± 0.9). Since this study does not address absolute rates or yield, for the sake of simplicity, most of reported reaction rates and yields are based on oxidized dimers only.

Chito-oligosaccharides resulting from the action of CBP21 on β-chitin were analyzed by hydrophilic interaction chromatography (HILIC) using a modified version[45] of a previously described UPLC method[1]. The elution of chito-oligosaccharides was monitored using an UV detector (205 nm).
All chromatograms were recorded using Chromeleon 7.0 software.

The production of H_2O_2 was measured by using the Amplex® Red Hydrogen Peroxide/Peroxidase Assay Kit from Thermo Fisher, with absorption monitoring at 540 nm, according to manufacturer's protocol.

Pre-activation experiments using the *hv*/V-TiO_2 system

A reaction mixture (300 µL) containing *Sc*LPMO10C (14 µM) and V-TiO_2 (5 g $.L^{-1}$) was exposed to light for 2 h, at 30 °C, with magnetic stirring, to reduce *Sc*LPMO10C-Cu(II) to *Sc*LPMO10C-Cu(I) (Reaction A). Prior to light exposure, the reaction mixture was flushed with nitrogen gas to minimize re-oxidation of the copper by oxygen. For all pre-activation experiments the irradiation was thus performed sidewise (1 cm distance from glass vial). Control reactions containing free Cu(II)SO_4 (5 µM, which is more than 7-fold the expected free Cu(II) concentration obtained when ScLPMO10C is part of the reaction, taking into account a K_d value of 31 nM[20]) or only sodium phosphate with V-TiO_2 (5 g $.L^{-1}$) were also prepared (reaction B and C). Control reactions containing *Sc*LPMO10C (14 µM), with or without V-TiO_2 (5 g $.L^{-1}$) incubated in the dark were also conducted (reactions E and F). After 2 hours exposure to visible light (I = 25%.I_{max}, 42 W.cm^{-2}) or storage in the dark, the reaction mixtures were centrifuged and the resulting supernatants were subsequently filtered to separate the electron source from the LPMO. A fraction (100

µL) of the filtrate was then added to a PASC suspension (100 µL, 0.56% w/v), prepared in-house according to a previously described method[46], in sodium phosphate (50 mM, pH 6.0) and pre-incubated at 40 °C for 30 min. For reactions B and C that did not contain enzyme during the pre-activation phase, fresh unexposed *Sc*LPMO10C-Cu(II) (to a final concentration of 7 µM) was added to the PASC solution to probe the reducing power in the filtrate. The filtrate from reaction D, which was identical to reaction C, was added to PASC without addition of enzyme to check for possible compounds generated during light-exposure of V-TiO_2 that could react with PASC. All PASC-containing reactions were incubated at 40 °C, 1000 rpm during 24 h, in the dark. Five PASC solutions (0.28 % final concentration w/v) in sodium phosphate (50 mM, pH 6.0) were also incubated at 40 °C, 1000 rpm, for 24 h to determine the background level of oxidized products.

From the filtrate of reactions A, E and F (see **Supplementary Fig. 9**) an activity test on PASC (0.28 % w/v) was performed using ascorbic acid as a reducing agent (1 mM) to ensure that the amount of catalytically operational enzyme (i.e. not denatured) was similar in all reactions (and thus ensure that the comparative analysis was valid). These reactions were also incubated at 40 °C, 1000 rpm, for 24 h.

After 24 h incubation, all samples were thermally treated (98 °C, 15 min) to inactivate the LPMO. Hydrolysis of the complete reaction mixture was then carried out by a mix of cellulases, *Tf*Cel5A endoglucanase (2 µM) and Cel7A cellobiohydrolase from *Trichoderma reesei* (*Tr*Cel7A, 2 µM) that were both purified in-house. After hydrolysis (45 °C, 24 h, 1000 rpm), oxidized products were analysed and quantified by HPAEC-PAD as described above. The background of oxidized product present in the PASC (83 ± 5 µM) was subtracted from all values displayed. Each experiment was carried out in triplicates.

The enzyme concentration of *Sc*LPMO10C was determined by measuring the absorbance at 280 nm of three different dilutions, using a molar extinction coefficient of 75,775 $M^{-1}.cm^{-1}$ as determined by the Protparam software.

For fluorescence analysis of the pre-activation step, two reaction glass vessels (1 mL volume each) were prepared for each of the four following set-ups: reactions (I) and (II) contained *Sc*LPMO10C (14 µM) in sodium phosphate buffer (50 mM, pH 6.0) and V-TiO_2 (5 $mg.mL^{-1}$), exposed to light (I = 25%.I_{max}, 42 $W.cm^2$) or kept in the dark, respectively. Reaction (III) was composed of only V-TiO_2 in sodium phosphate and exposed to light and reaction (IV) contained only *Sc*LPMO10C (14 µM) in sodium phosphate buffer (50 mM, pH 6.0) and was kept in the dark. All reactions were flushed with N_2 (3 min) prior to light exposure and then incubated during 2 h at room temperature under magnetic stirring and with application of light where applicable. After centrifugation (12,000 ×g, 2 min) in 1.5 mL Eppendorf tubes, supernatants were transferred to quartz cuvettes (the two 1 mL reactions of same kind were pooled to reach 2 mL final volume) after which fluorescence monitoring was immediately initiated. Reaction (III) constitutes a control to verify if the reducing power brought by light-exposed V-TiO_2 was efficiently removed from the solution by the centrifugation step/end of light exposure. For this, after the centrifugation step, fresh *Sc*LPMO10C (to 14 µM final concentration) was added to the supernatant to check if LPMO reduction took place. Reaction (IV) was used as a positive control to which ascorbic acid (5 µM) was added.

Fluorescence measurement for redox intermediate detection

Fluorescence signals were recorded using a Cary Eclipse Fluorescence spectrophotometer (Agilent Technologies) using a 2 mL reaction volume in quartz cuvettes (Hellma Analytics, 101-QS). During data

acquisition, solutions in the cuvettes were kept under magnetic stirring, at room temperature. After screening various excitation and emission wavelengths, the reduction of LPMOs was monitored by measuring the emission at 332 nm and an excitation wavelength of 282 nm, setting a PMT detector voltage at medium sensitivity (600 V).

Reaction mixtures containing ascorbic acid or the *hv*/V-TiO_2 system are described above. Reactions with L-cysteine or 1,4-dithiotreitol (DTT) as reducing agents (2, 100 or 1000 µM) were carried out with *Sc*LPMO10C (2 µM) in sodium phosphate (50 mM, pH 6.0).

The redox reaction initiated by reducing equivalents provided by the action of the cellobiose dehydrogenase from *Myriococcum thermophilum* (*Mt*CDH, 0.25 µM) on lactose (1 mM) was carried out with wild-type CBP21, or its H114A mutant (each at 2 µM), that were produced and purified as previously described[26]. Recombinant *Mt*CDH was produced as a His-tagged protein in *Pichia pastoris* and purified by IMAC using standard Ni-NTA affinity resin. To decrease the signal intensity due to the presence of *Mt*CDH the PMT detector voltage was set to 550 mV.

References

1. Vaaje-Kolstad, G. *et al.* An oxidative enzyme boosting the enzymatic conversion of recalcitrant polysaccharides. *Science* **330,** 219–222 (2010).
2. Forsberg, Z. *et al.* Cleavage of cellulose by a CBM33 protein. *Protein Sci.* **20,** 1479–1483 (2011).
3. Quinlan, R. J. *et al.* Insights into the oxidative degradation of cellulose by a copper metalloenzyme that exploits biomass components. *Proc. Natl. Acad. Sci. U. S. A.* **108,** 15079–15084 (2011).
4. Phillips, C. M., Beeson, W. T., Cate, J. H. & Marletta, M. A. Cellobiose dehydrogenase and a copper-dependent polysaccharide monooxygenase potentiate cellulose degradation by *Neurospora crassa*. *ACS Chem. Biol.* **6,** 1399–1406 (2011).
5. Agger, J. W. *et al.* Discovery of LPMO activity on hemicelluloses shows the importance of oxidative processes in plant cell wall degradation. *Proc. Natl. Acad. Sci. U. S. A.* **111,** 6287–6292 (2014).
6. Vu, V. V, Beeson, W. T., Span, E. A., Farquhar, E. R. & Marletta, M. A. A family of starch-active polysaccharide monooxygenases. *Proc. Natl. Acad. Sci. U. S. A.* **111,** 13822–13827 (2014).
7. Kim, S., Ståhlberg, J., Sandgren, M., Paton, R. S. & Beckham, G. T. Quantum mechanical calculations suggest that lytic polysaccharide monooxygenases use a copper-oxyl, oxygen-rebound mechanism. *Proc. Natl. Acad. Sci. U. S. A.* **111,** 149–154 (2014).
8. Kjaergaard, C. H. *et al.* Spectroscopic and computational insight into the activation of O_2 by the mononuclear Cu center in polysaccharide monooxygenases. *Proc. Natl. Acad. Sci. U. S. A.* **111,** 8797–8802 (2014).
9. Rodríguez-Zúñiga, U. F. *et al.* Lignocellulose pretreatment technologies affect the level of enzymatic cellulose oxidation by LPMO. *Green Chem.* **17,** 2896–2903 (2015).
10. Westereng, B. *et al.* Enzymatic cellulose oxidation is linked to lignin by long-range electron transfer. *Sci. Rep.* **5,** 18561 (2015).
11. Langston, J. A. *et al.* Oxidoreductive cellulose depolymerization by the enzymes cellobiose dehydrogenase and glycoside hydrolase 61. *Appl. Environ. Microbiol.* **77,** 7007–7015 (2011).
12. Kittl, R., Kracher, D., Burgstaller, D., Haltrich, D. & Ludwig, R. Production of four *Neurospora crassa* lytic polysaccharide monooxygenases in *Pichia pastoris* monitored by a fluorimetric assay. *Biotechnol. Biofuels* **5,** 79 (2012).
13. Ludwig, R., Harreither, W., Tasca, F. & Gorton, L. Cellobiose dehydrogenase: A versatile catalyst for electrochemical applications. *ChemPhysChem* **11,** 2674–2697 (2010).
14. Wandrey, C. Biochemical reaction engineering for redox reactions. *Chem. Rec.* **4,** 254–265 (2004).
15. Narayanam, J. M. R. & Stephenson, C. R. J. Visible light photoredox catalysis: applications in organic synthesis. *Chem. Soc. Rev.* **40,** 102–113 (2011).
16. Maciá-Agulló, J. A., Corma, A. & Garcia, H. Photobiocatalysis: the power of combining photocatalysis and enzymes. *Chemistry* **21,** 10940–10959 (2015).
17. Mifsud, M. *et al.* Photobiocatalytic chemistry of oxidoreductases using water as the electron donor. *Nat. Commun.* **5,** 3145 (2014).
18. Hashimoto, K., Irie, H. & Fujishima, A. TiO_2 Photocatalysis: A historical overview and future prospects. *Jpn. J. Appl. Phys.* **44,** 8269–8285 (2005).
19. Ni, M., Leung, M. K. H., Leung, D. Y. C. & Sumathy, K. A review and recent developments in photocatalytic water-splitting using TiO_2 for hydrogen production. *Renew. Sustain. Energy Rev.* **11,** 401–425 (2007).
20. Forsberg, Z. *et al.* Structural and functional characterization of a conserved pair of bacterial cellulose-oxidizing lytic polysaccharide monooxygenases. *Proc. Natl. Acad. Sci. U. S. A.* **111,** 8446–8451 (2014).
21. Walling, C. Fenton reagent revisited. *ACC Chem. Res.* **8,** 125–131 (1975).
22. Goldstein, S., Meyerstein, D. & Czapski, G. The Fenton reagents. *Free Radic. Biol. Med.* **15,** 435–445 (1993).
23. Sheng, H., Ji, H., Ma, W., Chen, C. & Zhao, J. Direct four-electron reduction of O_2 to H_2O on TiO_2 surfaces by pendant proton relay. *Angew. Chemie - Int. Ed.* **52,** 9686–9690 (2013).
24. Goldberg, M. & Pecht, I. Fluorescence enhancement of laccase induced by reduction of Cu(II) Sites. *Proc. Natl. Acad. Sci.* **71,** 4684–4687 (1974).
25. Tepper, A. W. J. W., Bubacco, L. & Canters, G. W. Stopped-flow fluorescence studies of inhibitor binding to tyrosinase from *Streptomyces antibioticus*. *J. Biol. Chem.* **279,** 13425–13434 (2004).
26. Vaaje-Kolstad, G., Horn, S. J., van Aalten, D. M. F., Synstad, B. & Eijsink, V. G. H. The non-catalytic chitin-binding protein CBP21 from *Serratia marcescens* is essential for chitin degradation. *J. Biol. Chem.* **280,** 28492–28497 (2005).
27. Fujishima, A. & Honda, K. Electrochemical photolysis of water at a semiconductor electrode. *Nature* **238,** 37–38 (1972).
28. Connor, P. A. & McQuillan, A. J. Phosphate adsorption onto TiO_2 from aqueous solutions: An *in situ* internal reflection infrared spectroscopic study. *Langmuir* **15,** 2916–2921 (1999).
29. He, T. *et al.* Bio-template mediated *in situ* phosphate transfer to hierarchically porous TiO_2 with localized phosphate distribution and enhanced photoactivities. *J. Phys. Chem. C* **118,** 4607–4617 (2014).

30. Luan, P. *et al.* Improved photoactivity of TiO_2-Fe_2O_3 nanocomposites for visible-light water splitting after phosphate bridging and its mechanism. *Phys. Chem. Chem. Phys.* **17,** 5043–5050 (2015).
31. Kang, S. A., Li, W., Lee, H. E., Phillips, B. L. & Lee, Y. J. Phosphate uptake by TiO_2: Batch studies and NMR spectroscopic evidence for multisite adsorption. *J. Colloid Interface Sci.* **364,** 455–461 (2011).
32. Frederiksen, R. F. *et al.* Bacterial chitinases and chitin-binding proteins as virulence factors. *Microbiology* **159,** 833–847 (2013).
33. Xu, C., Spadiut, O., Araújo, A. C., Nakhai, A. & Brumer, H. Chemo-enzymatic assembly of clickable cellulose surfaces via multivalent polysaccharides. *ChemSusChem* **5,** 661–665 (2012).
34. Holtmann, D., Fraaije, M. W., Arends, I. W. C. E., Opperman, D. J. & Hollmann, F. The taming of oxygen: biocatalytic oxyfunctionalisations. *Chem. Commun. (Camb).* **50,** 13180–13200 (2014).
35. Kumar, S. G. & Devi, L. G. Review on modified TiO_2 photocatalysis under UV / visible light : selected results and related mechanisms on interfacial charge carrier transfer dynamics. *J. Phys. Chem. A* **115,** 13211–13241 (2011).
36. Guo, Q. *et al.* Elementary photocatalytic chemistry on TiO_2 surfaces. *Chem. Soc. Rev.* (2016).
37. Ran, J., Zhang, J., Yu, J., Jaroniec, M. & Qiao, S. Z. Earth-abundant cocatalysts for semiconductor-based photocatalytic water splitting. *Chem. Soc. Rev.* **43,** 7787–7812 (2014).
38. Lee, J. Y. & Karlin, K. D. Elaboration of copper-oxygen mediated CH activation chemistry in consideration of future fuel and feedstock generation. *Curr. Opin. Chem. Biol.* **25,** 184–193 (2015).
39. Beeson, W. T., Vu, V. V., Span, E. A., Phillips, C. M. & Marletta, M. A. Cellulose degradation by polysaccharide monooxygenases. *Annu. Rev. Biochem.* **84,** 923–946 (2014).
40. Borisova, A. S. *et al.* Structural and functional characterization of a lytic polysaccharide monooxygenase with broad substrate specificity. *J. Biol. Chem.* **290,** 22955–22969 (2015).
41. Choudhury, S., Baeg, J.-O., Park, N.-J. & Yadav, R. K. A solar light-driven, eco-friendly protocol for highly enantioselective synthesis of chiral alcohols via photocatalytic/biocatalytic cascades. *Green Chem.* **16,** 4389 (2014).
42. Choi, S. H. *et al.* The influence of non-stoichiometric species of V/TiO_2 catalysts on selective catalytic reduction at low temperature. *J. Mol. Catal. A Chem.* **304,** 166–173 (2009).
43. Westereng, B. *et al.* The putative endoglucanase *Pc*GH61D from *Phanerochaete chrysosporium* is a metal-dependent oxidative enzyme that cleaves cellulose. *PLoS One* **6,** e27807 (2011).
44. Westereng, B., Wittrup, J., Horn, S. J. & Vaaje-Kolstad, G. Efficient separation of oxidized cello-oligosaccharides generated by cellulose degrading lytic polysaccharide monooxygenases. *J. Chromatogr. A* **1271,** 144–152 (2013).
45. Loose, J. S. M., Forsberg, Z., Fraaje, M. W., Eijsink, V. G. H. & Vaaje-Kolstad, G. A rapid quantitative activity assay shows that the *Vibrio cholerae* colonization factor GbpA is an active lytic polysaccharide monooxygenase. *FEBS Lett.* 6–11 (2014).
46. Wood, T. M. *Biomass Part A: Cellulose and Hemicellulose*. *Methods in Enzymology* **160,** (Elsevier, 1988).

Aknowledgement

We thank Bjørge Westereng at NMBU, Ås and Mats Sandgren at SLU, Uppsala, Sweden for providing a sample of a purified recombinant fungal AA9 (*Pc*LPMO9D). We thank Roland Ludwig at BOKU, Vienna, Austria for providing us with *Mt*CDH. This work was funded by the Research Council of Norway through grant 214613, the VISTA programme of the Norwegian Academy of Science and Letters, through grant 6510. B.B. has received the support of the EU in the framework of the Marie-Curie FP7 COFUND People Programme, through the award of an AgreenSkills fellowship (under grant agreement n° 267196). The postdoctoral fellowship of B.B. was also supported by the French Institut National de la Recherche Agronomique (INRA) [CJS].

Author contributions

B.B. designed and performed the photobiocatalytic experiments, conceived and performed pre-activation and fluorescence experiments, analysed the results and wrote the manuscript. N.Y. prepared the photocatalyst. Z.F. and G.V.-K. provided enzymes, and contributed to the analysis of the experiments and to writing of the manuscript. F.H. and V.G.H.E. conceived the study, developed the photobiocatalytic concept, analysed data and contributed to writing of the manuscript.

Competing financial interest

The authors declare to have no competing interests as defined by Nature Publishing Group, or other interests that might be perceived to influence the results and/or discussion reported in this article.

Additional information

Supplementary information and methods are available online.